# *сверхпроводимость и магнетизм в нецентросимметричном соединении* RhGe (B20)

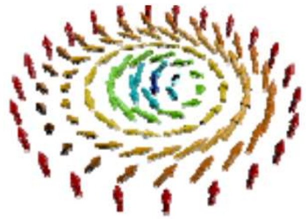

*ИФВД РАН:* <u>Цвященко А.В.,</u> Сидоров В.А., Петрова А.Е., Фомичева Л.Н., Зибров И.П.
*ИК РАН:* Дмитриенко В.Е.

# Введение: кубические фазы высокого давления (B20) в системе MnGe-RhGe

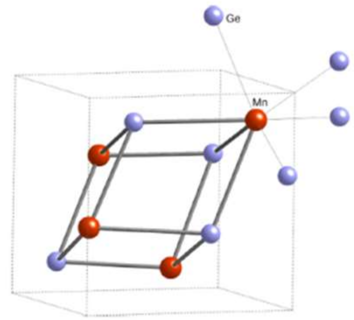


- Впервые при высоком давлении синтез германидов с d- металлами ($W_5Ge_3$ и $WGe_2$) был проведен в ИФВД в конце *семидесятых* годов.

-- S.V. Popova, L.N. Fomicheva. Phase transitions in intermetallic compounds under : synthesis of tungsten germanides. High-Pressure science and technology. Sixth AIRAPT Conference, 1977, v.1, New-York – London, 272-273.

-- С.В. Попова, Л.Н. Фомичева, Синтез германидов вольфрама при высоком давлении. Известия АН СССР. Неорганические материалы, 1978, т. 14, № 4, 684-686.

- В начале *восьмидесятых* гг. впервые при высоком давлении были синтезированы моногерманид кобальта и родия (**CoGe , RhGe**) с кубической структурой без центра инверсии B20.

-- V.I. Larchev, S.V. Popova, The polymorphism of transition metal monogermanides at high pressures and temperatures. *Journal of the Less-Common Metals*, 87, 53-57 (1982).

Синтез германидов проводился в камере типа «тороид», разработанной в ИФВД

-- L.G. Khvostantsev, V.N. Slesarev and V.V. Brazhkin, High Pressure Research, 24, 371 (2004).

- И только в конце *восьмидесятых* японской группой были синтезированы моногерманиды марганца и кобальта (MnGe, CoGe) со структурой B20.

-- H. Takizawa, T. Sato, T. Endo and M. Shimada, High-Pressure Synthesis and Electrical and Magnetic Properties **MnGe** and **CoGe** with the Cubic B20 Structure, Journal of Solid State Chemistry,73, 40 (1988).

1. N. Kanazawa, Y. Onose, T. Arima, D. Okuyama, K. Ohoyama, S.Wakimoto, K. Kakurai, S. Ishiwata, and Y. Tokura, *"Large Topological Hall Effect in a Short-Period Helimagnet MnGe"* Phys. Rev. Lett. **106**, 156603 (2011).
2. O. L. Makarova, A. V. Tsvyashchenko, G. Andre, F. Porcher, L. N. Fomicheva, N. Rey, and I. Mirebeau, "*Neutron diffraction study of the chiral magnet MnGe*" Phys. Rev. B **85**, 205205 (2012).

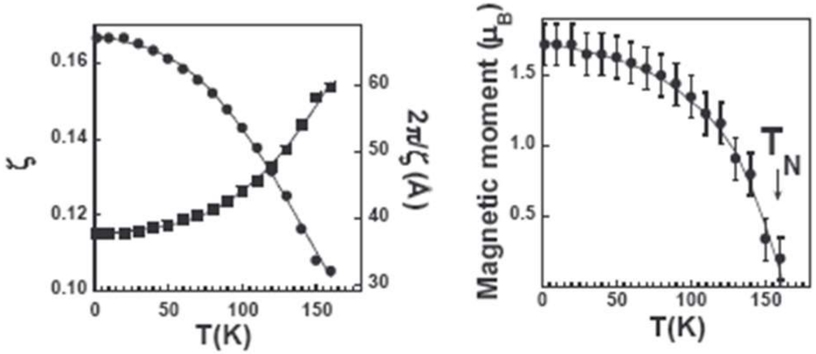


left: temperature variations of the  component of the wavevector k=2π/a (0, 0, ζ) where $\zeta = 0.107(5)$ just below the transition temperature $T_N = 170$ K. and period of the spiral for MnGe; The ζ value increases upon cooling and locks in to the value of 0.167(4) below 30 K.
right: temperature dependence of the ordered Mn magnetic moment.

Phys. Rev.B 89, 180407(R) (2014)

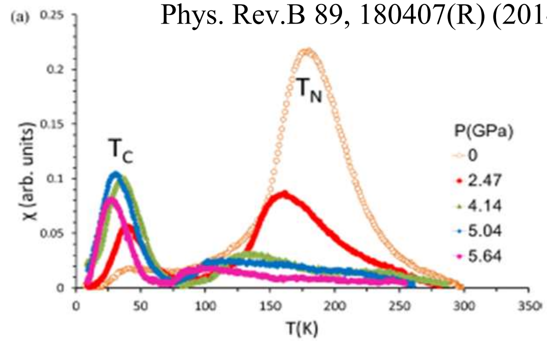


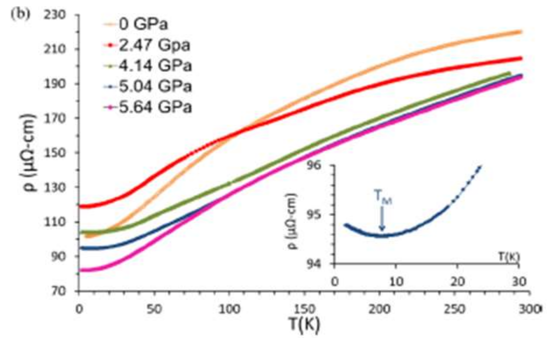


arXiv:1601.05332v 20Jan (2016)

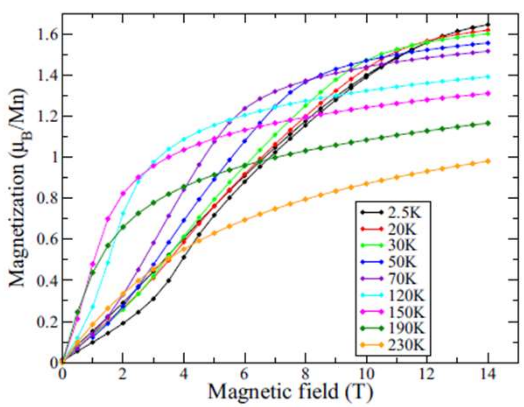


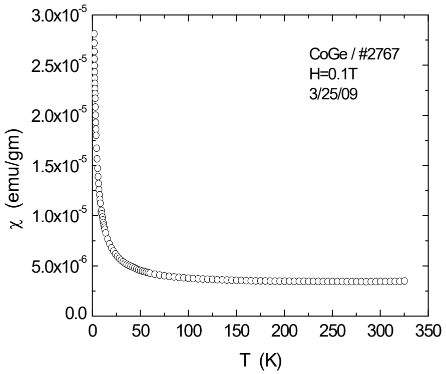


*Solid State Phenomena Vol. 190 (2012) pp 225-228*

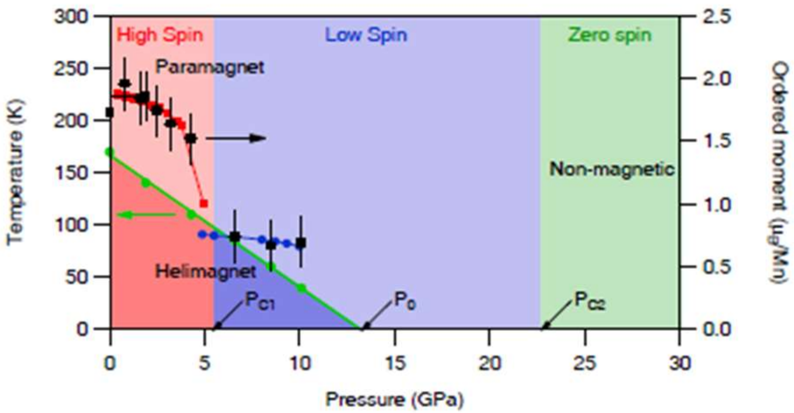

# Параметры решетки, температурные зависимости восприимчивости и намагниченности соединений $Mn_{(1-x)}Rh_{(x)}Ge$

$Mn_{1-x}Fe_xGe$ - Phys. Rev. Letters 110, 207201, 17 MAY (2013)

$Fe_{1-x}Co_xGe$ - Phys. Rev. B 90, 174414 (2014)

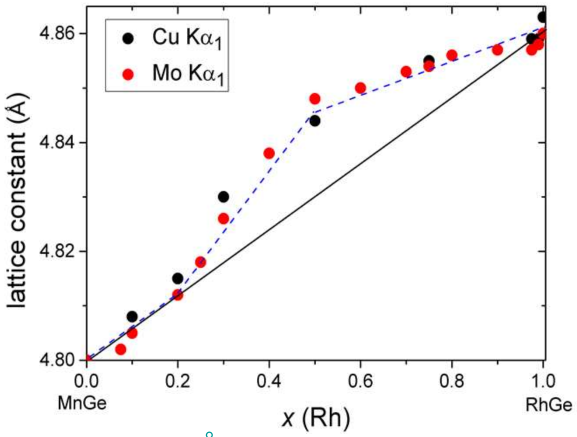


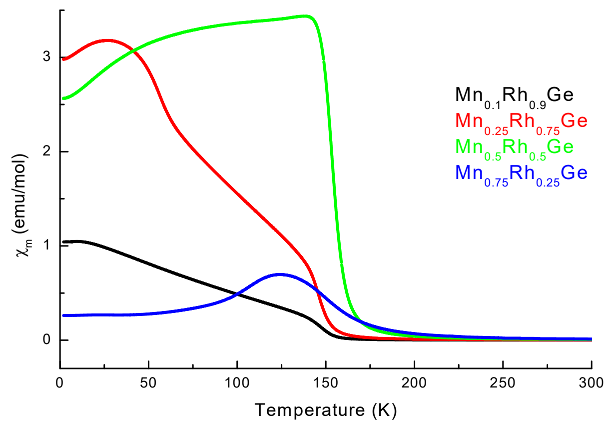


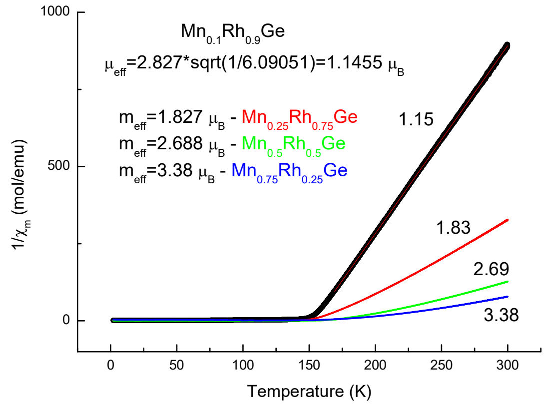


RuGe a= 4.846 Å

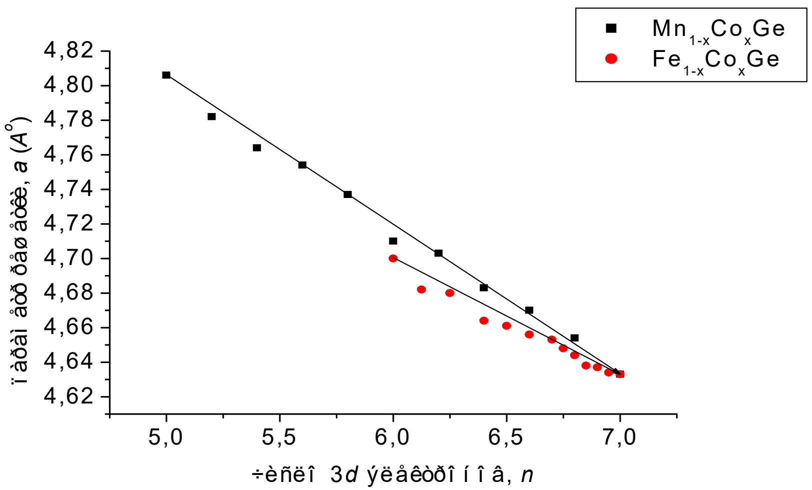


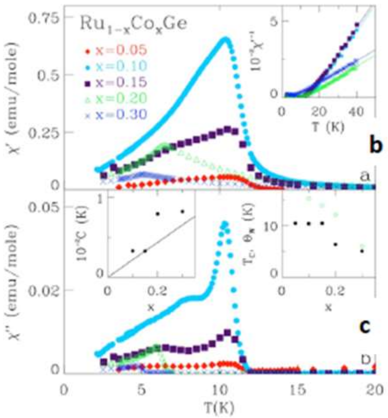


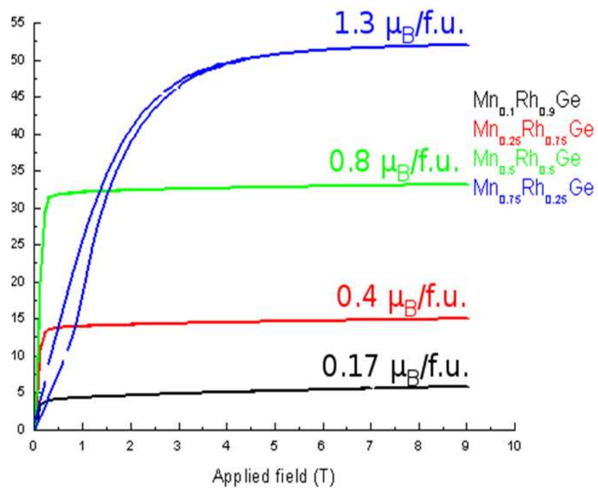

# Синтез и структура RhGe (B20)

Вид образца после плавления исходной смеси Rh (99.99%) и Ge (99.999%) при высоком давлении 8 ГПа в контейнере из NaCl.

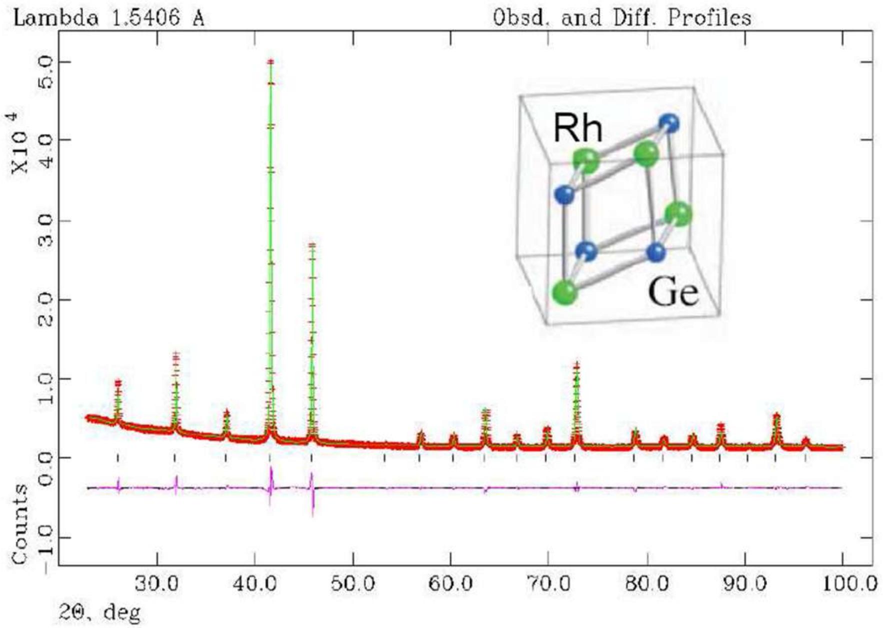


X-ray powder diffraction pattern from $RhGe_{0.986}$ (RF = 0.0188, RP = 0.0260, RWP = 0.0418). (+): measured diffraction pattern, (solid line): Rietveld refinement and (bottom curve): the difference between the two dependencies. The positions of allowed Bragg reflections are indicated by vertical tick marks. Inset: the crystal structure of B20-type RhGe space group $P2_13$ (No..198) with $a$ =4.85954(2) °A ($V$ = 114.758(1) °$A^3$)

# Heavy Fermion Superconductivity and Magnetic Order in Noncentrosymmetric $CePt_3Si$

space group *P4mm (No. 99)*

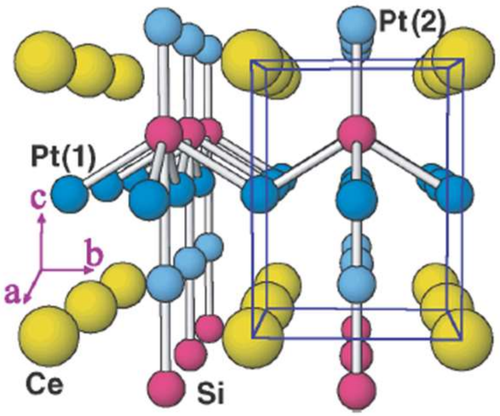


$T_N \approx 2.2$ K
$T_{SC} \approx 0.7$ K

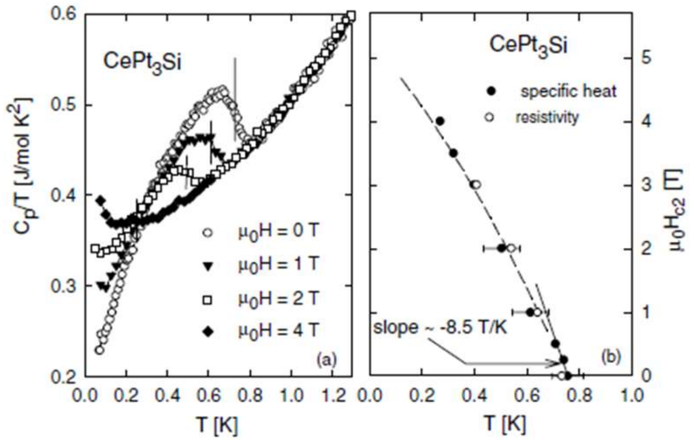



E. Bauer,[1] G. Hilscher,[1] H. Michor,[1] Ch. Paul,[1] E.W. Scheidt,[2] A. Gribanov,[3] Yu. Seropegin,[3] H. Noël,[4] M. Sigrist,[5] and P. Rogl[6]



VOLUME 92, NUMBER 2 PHYSICAL REVIEW LETTERS week ending 16 JANUARY 2004


V.M. Edelstein, Zh. E . ksp. Teor. Fiz. **95, 2151 (**1989)@JETP 68, 1244 (1989); V.M. Edelstein, Phys. Rev. Lett. **75, 2004** (1995).
L.P. Gor'kov and E.I. Rashba, Phys. Rev. Lett. **87, 037004** (2001).
According to V.M. Edelstein and L.P. Gor'kov and E.I. Rashba, in the absence of inversion symmetry the order parameter becomes a mixture of spin-singlet and spin-triplet components

C. Pfleiderer, G. J. McMullan, S. R. Julian, and G. G. Lonzarich, Phys. Rev. B 55, 8330 (1997).
Ожидали сверхпроводимость при высоком давлении в зонном магнетике MnSi (B20), но наблюдали только магнетизм.

# Температурные зависимости сопротивления теплоемкости и восприимчивости RhGe

We estimated $dH_{c2}/dT$ at $T_c$ as $-0.65$ kOe/K.

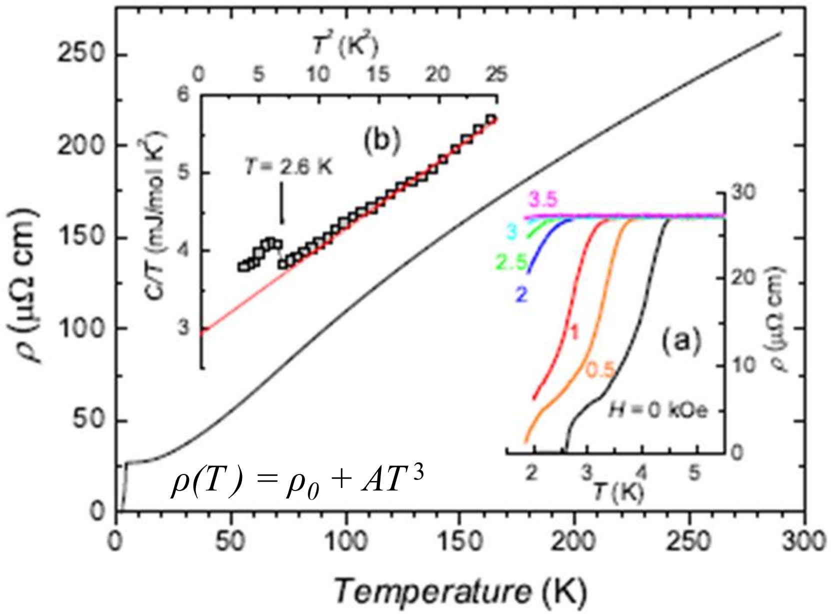


Temperature dependence of the electrical resistivity of RhGe0.986. Inset (a) - temperature dependences of resistivity in various magnetic fields around the superconducting transition. Inset (b) - temperature dependence of the specific heat (in the form C/T vs T $^2$) of RhGe around the superconducting transition.

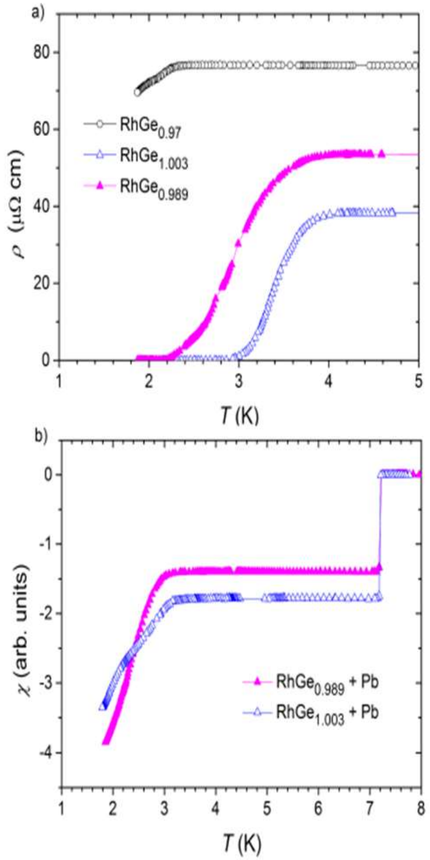


a) Temperature dependence of the electrical resistivity of RhGe at various filling of the Ge-site.

b) Temperature dependence of the magnetic susceptibility of RhGe and a piece of Pb with external dimensions close to those of RhGe sample at various filling of the Ge-site.

$\gamma = 2.9$ mJ/(mol·K$^2$)

In RhGe the jump $\Delta C/\gamma T_c \sim 0.16$ The BCS value ($\Delta C/\gamma T_c = 1.43$).

Similar small jump C/γTc = 0.25 was found in the noncentrosymmetric antiferromagnetic superconductor CePt3Si

# Спектры дифференциальной проводимости *G=dI/dV* RhGe

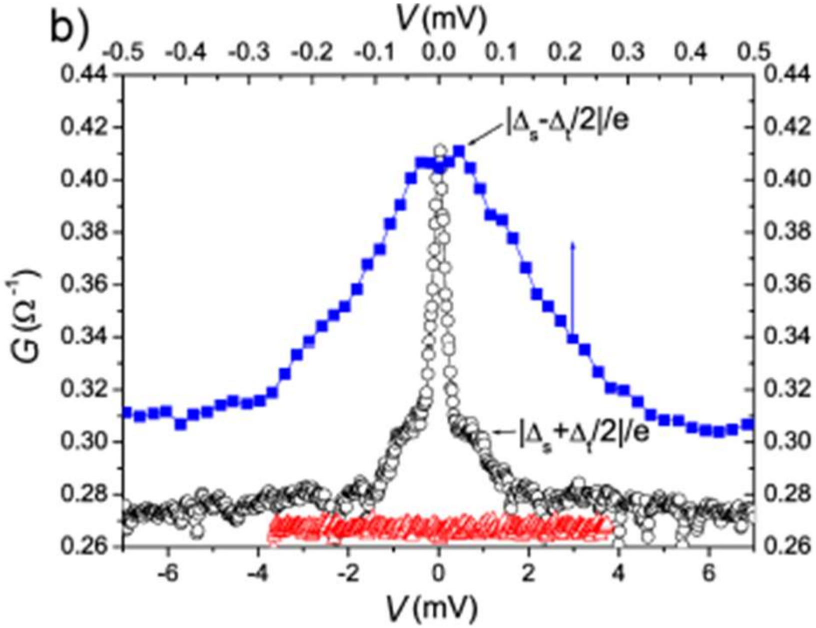


(○)-the Andreev signal of RhGe0.986 in the superconducting state at ambient pressure and at 1.8 K. (Δ)-the conductance of contact in the normal state at 4.3 K. The bold squares are the enlarged central part of spectrum taken at T = 1.8 K. The characteristic bumps of spectrum located at bias voltages $V = |\Delta_s \pm \Delta_{t/2}|/e$ according to Ref.[Linder] are marked by arrows (the bumps at $V_1 \approx 0.03$ mV , $V_2 \approx 0.96$ mV and the gaps $\Delta_s \approx 0.46$ meV and $\Delta_t \approx 0.93$ meV and the triplet component dominates.

In the absence of an inversion center the spectrum of Cooper pairs can have two energy gaps and the order parameter contains not only a singlet part, but also an admixture of a triplet state, whereas the zero-temperature spin susceptibility is finite. (V.M. Edelstein -1989)

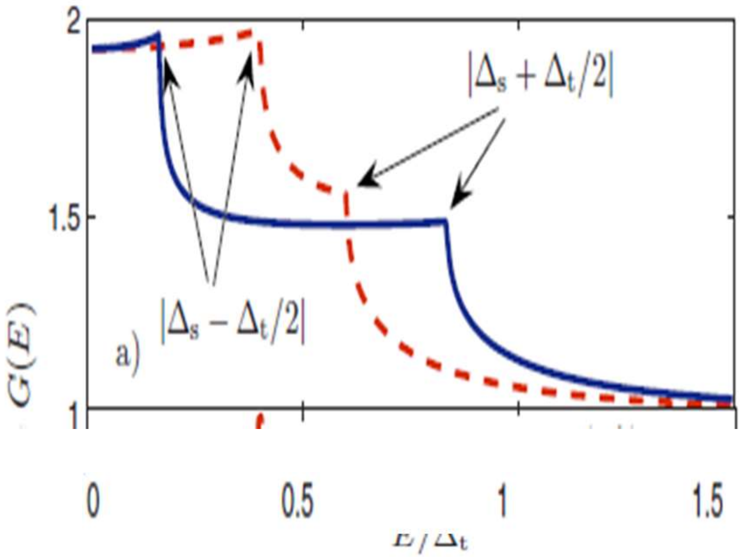


It is seen that the conductance spectra reveal information about the relative size of the singlet and triplet components of the gaps by characteristic features located at bias voltages $E=\Delta_s \pm \Delta_{t/2}$.

J.Linder and A. Sudbo
Quantum transport in noncentrosymmetric superconductors and thermodynamics of ferromagnetic superconductors
Phys. Rew. B 76, 054511 (2007)

# Температурная зависимость магнитной восприимчивости и полевая зависимость намагниченности RhGe

$T_m \sim 140$ K

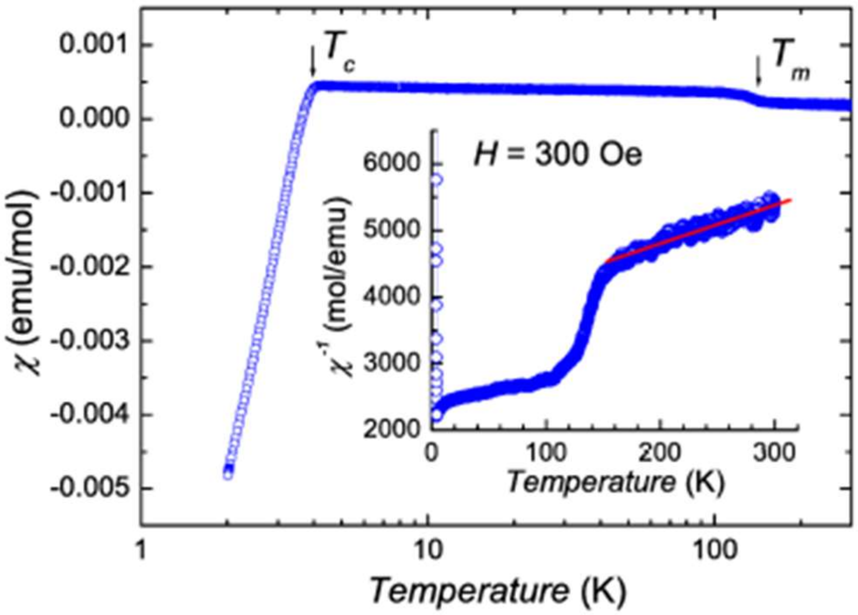


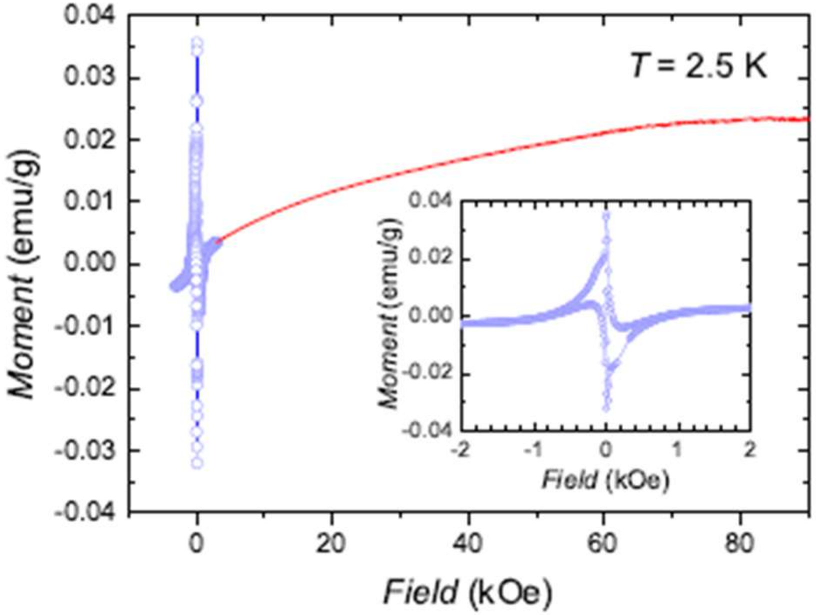


$\mu_{eff} = 1.18\ \mu_B$/f.u.

$M_S \sim 0.001\ \mu_B$/f.u.

# Временные спектры угловой анизотропии, измеренные методом ВУК на ядрах $^{111}$Cd в RhGe

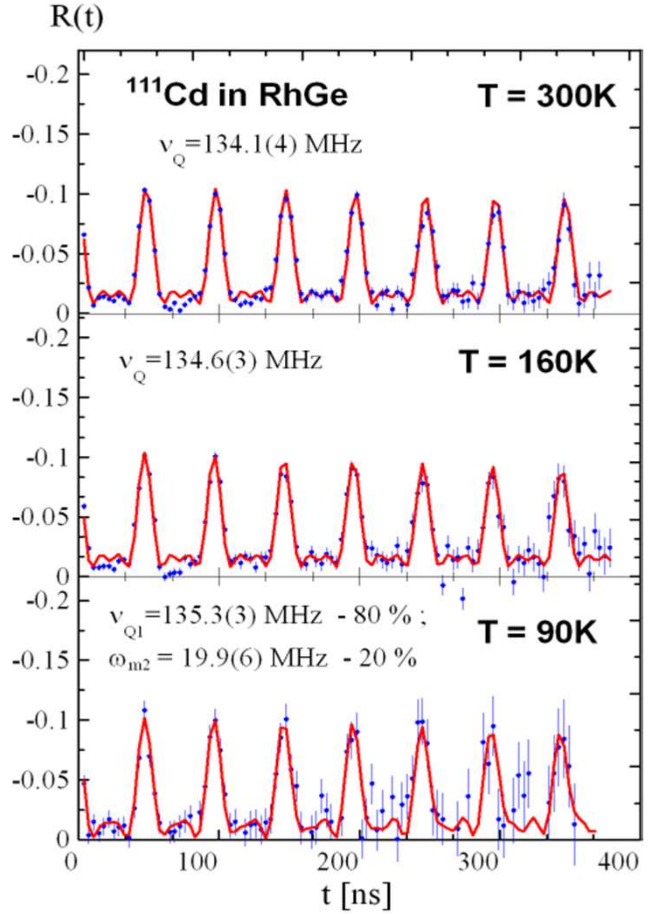


$^{57}$Fe in MnGe

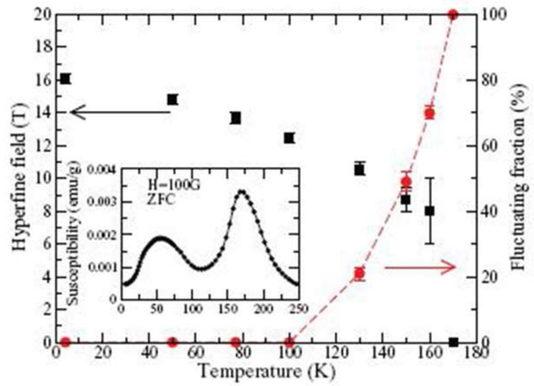


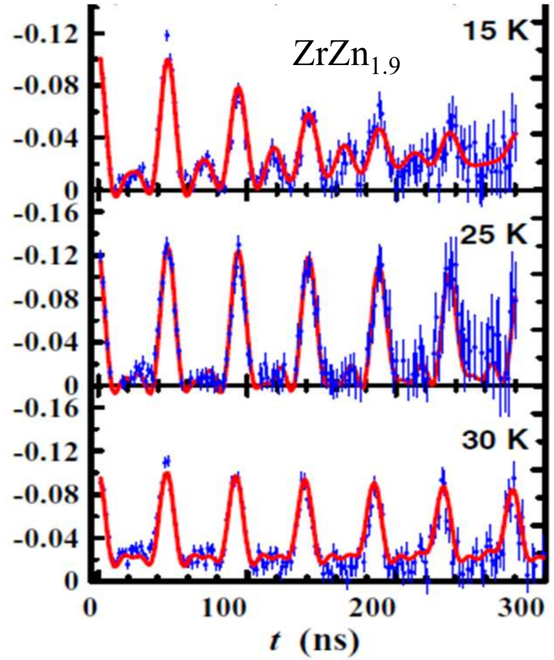


Time spectra of the angular correlation anisotropy, *R(t)* for $^{111}$Cd in $ZrZn_{1.9}$ measured at various temperatures and normal pressure ($T_C = 29$ *K*).

The EFG $V_{zz} = v_Q h/eQ = 6.7(2) \times 10^{17}$ V/sm$^2$

the magnetic hyperfine field $B = 8.6(1)$ T ($B_{HF} = 2\pi v_L/g\mu_N$)

The EFG $V_{zz} = 7.0(2) \times 10^{17}$ V/sm$^2$

$B_{Zr} = 9.2(1)$ T

# Зависимость температуры сверхпроводящего перехода от давления для нецентоносимметричных RhGe и $RhGe_4$

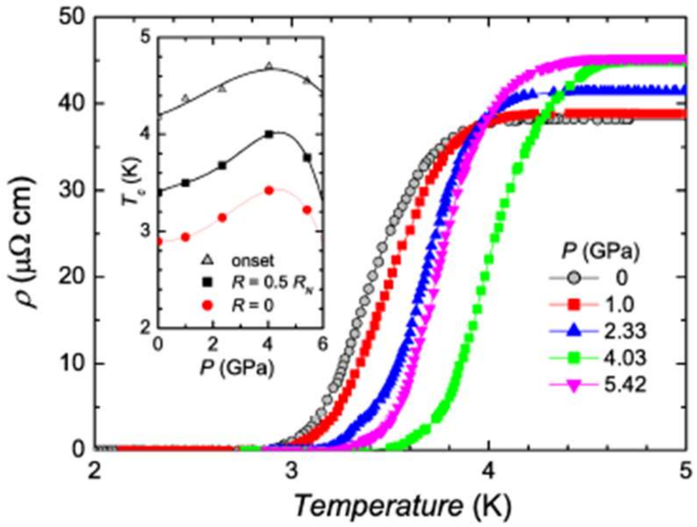


Temperature dependence of the electrical resistivity of $RhGe_{1.003}$ near the superconducting transition at various pressures. The inset shows the P-T diagram of superconductivity in RhGe ($P2_13$ ).

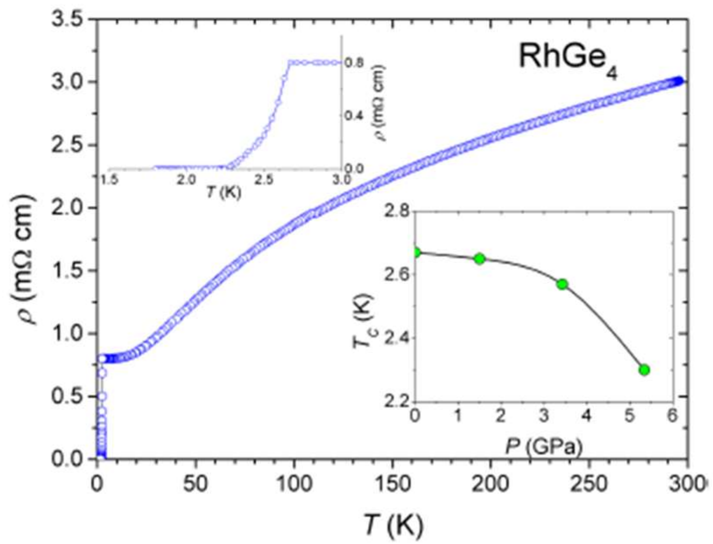


Temperature dependence of the electrical resistivity of $RhGe_4$(superconducting phase with structure of $IrGe_4$-type synthesized under high pressure [Larchev, Popova]) near the superconducting transition at ambient pressure. The inset shows the P-T diagram of superconductivity in trigonal $RhGe_4$. **Space Group:** 152 ($P3_121$), $Z$=3

# Структура, электронные и магнитные свойства: оценка с использованием расчётов ab initio на примере QUANTUM ESPRESSO

RhGe (B20) space group *$P2_13$* (No..198) with $a$ =4.85954(2) °A ($V$ = 114.758(1) °$A^3$)

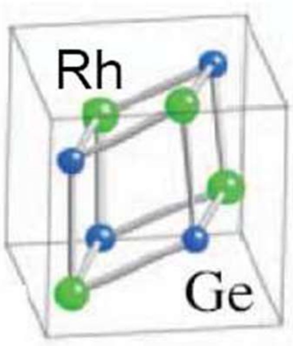


←

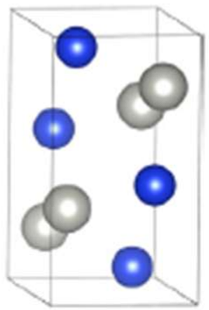

**FeSi** **MnP**

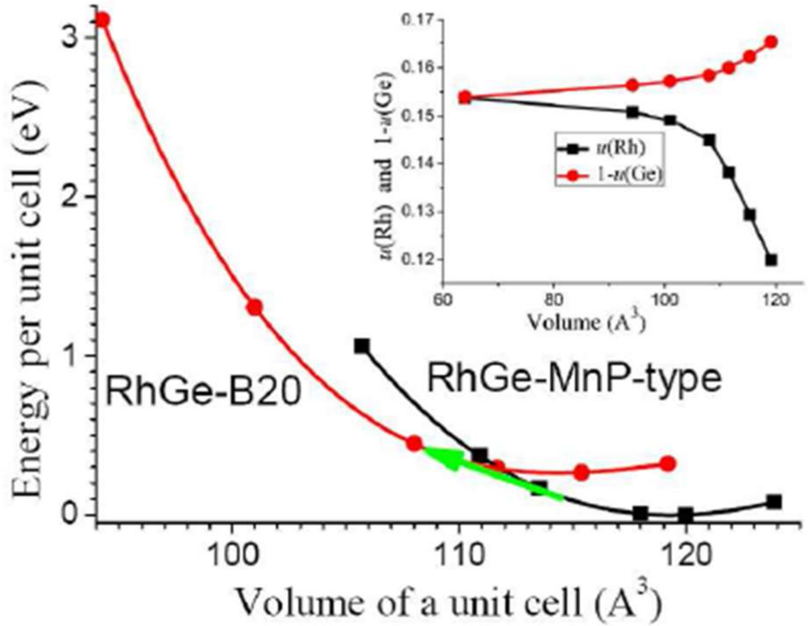


RhGe (B31) space group *Pnma* (No..62) with $V$ = 119.273 (2) °$A^3$ ΔV/V = 0.038

RhGe *Pnma* (No. 62) $wR_2 = 0.0211$, $R_1 = 0.0101$
$a = 5.704(2)$ Å, $b = 3.215(1)$ Å, $c = 6.504(2)$ Å

| Atom | Site | $x$ | $y$ | $z$ |
|---|---|---|---|---|
| Rh | 4$c$ | 0.00339(4) | 1/2 | 0.20193(4) |
| Ge | 4$c$ | 0.19144(6) | 1/2 | 0.93977(5) |
| | $U_{11}$ | $U_{22}$ | $U_{33}$ | |
| Rh | 0.0023(2) | 0.0051(2) | 0.0035(2) | |
| Ge | 0.0030(2) | 0.0044(2) | 0.0041(2) | |

Calculated total energy vs the unit cell volume for metastable (B20) and stable (MnP-type) phases of RhGe. The tangent line (green arrow) determines the transition pressure (about 8 GPa) and the volume change at the transition point (about 6%). Zero energy corresponds to the MnP-type phase at zero pressure. Inset: changes of the Rh and Ge lattice parameters u in the B20 phase.

# Намагниченность **M** в кристалле MnGe и RhGe при нормальном давлении (QUANTUM ESPRESSO)

MnGe

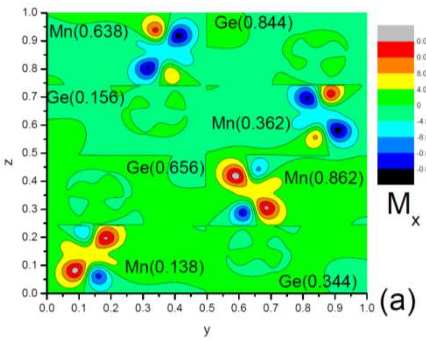


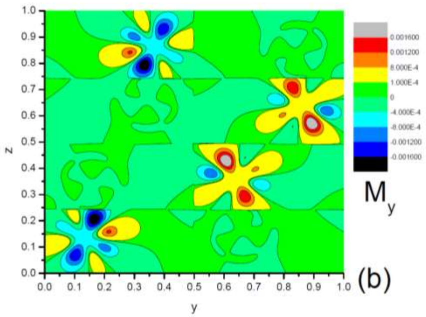


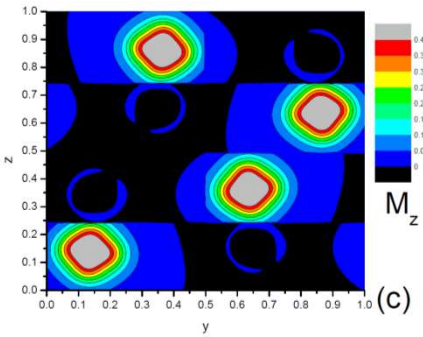


RhGe

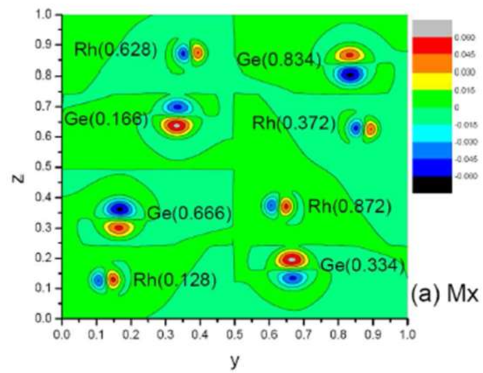


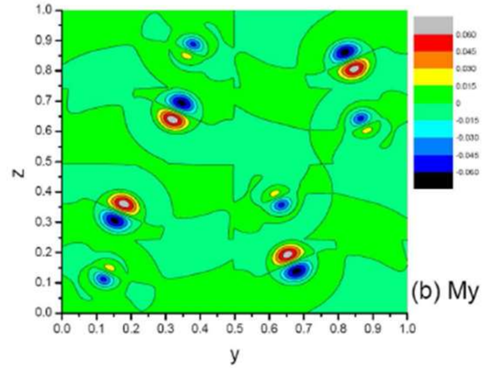


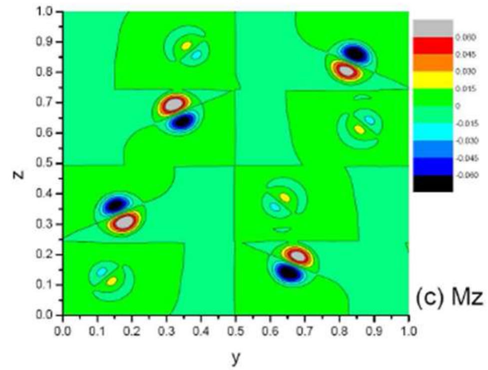


The calculated total magnetization is rather small and directed along the z−axis, $|\langle M(r)\rangle| \approx 0.0077\ \mu_B$, whereas the average absolute magnetization $\langle|M(r)|\rangle \approx 1.0\ \mu$B.

Распределение компоненты $M_x$ и $M_y$ неколлинеарного магнитного момента в элементарной ячейке MnGe и RhGe. Координаты атомов перпендикулярно поверхности рисунка показаны цифрами в скобках. Цветная палитра в правой части рисунка показывает величину и направление этой компоненты.

Распределение компоненты $M_z$ неколлинеарного магнитного момента в элементарной ячейке MnGe и RhGe. Отметим, что z-компонента MnGe сконцентрирована на атомах **марганца** и более чем в 200 раз превышает x и y компоненты.

## Некоторые выводы из расчетов магнитных свойств

For quantitative characterization of atomic magnetization we consider different quantities integrated over small spheres around the atom . The radius of the spheres was chosen as 0.64 Å. The total volume of 8 spheres is only 7.8% of the unit cell.

1-We have found that the atomic magnetization vector averaged over the sphere is $\langle \mathbf{M}(r) \rangle_{sph} = (170, 55, 20) \cdot 10^{-4} \mu_B$ for Rh and $(2,-4,-3) \cdot 10^{-4} \mu_B$ for Ge.

2-The absolute magnetization inside the spheres gives only 40% of the absolute magnetization, $\langle |\mathbf{M}(r)| \rangle_{sph} = 0.04 \mu_B$ per Rh and 0.06 $\mu_B$ per Ge.

3-The spatial distribution of magnetization inside the atomic spheres can be also characterized by a non-symmetric tensor $Q_{jk} = \langle r_j M'_k \rangle_{sph}$ where **r** is the dimensionless radius vector inside the unit cell and
$\mathbf{M}'(r) = \mathbf{M}(r) - \langle \mathbf{M}(r) \rangle_{sph}$. This tensor violates both $T$ - and $P$-invariance [I. Dzyaloshinskii, Solid State Comm. 82, 579 (1992)] and can appear, for instance, if a p-state is admixed to an s-state. The symmetric part $(Q_{jk}+Q_{kj})/2$ is the magnetic quadrupole moment of the atom and the antisymmetric part $(Q_{jk} - Q_{kj})/2$ is equivalent to the vector of atomic toroidal moment $\mathbf{T} = \langle \mathbf{r} \times \mathbf{M}'(\mathbf{r}) \rangle_{sph}$. It is interesting that there is a non-zero scalar part $Q_{jj}$ arising from the spin hedgehog pattern around each atom : $Q_{jj}$ is about $1.5 \cdot 10^{-4}\ \mu_B$ for Rh (plus for the two atoms and minus for another two) and $1.0 \cdot 10^{-4}\ \mu_B$ for Ge. Thus each atom in RhGe has a complicated magnetic pattern and can be considered as an atomic-size Skyrmion. The calculated toroidal moment for Rh is of about $2.6 \cdot 10^{-4} \mu_B$ whereas for Ge it is only $0.2 \cdot 10^{-4} \mu_B$.

# Топологические решетки узлов с нулевой намагниченностью

The meron-anti-meron lattice

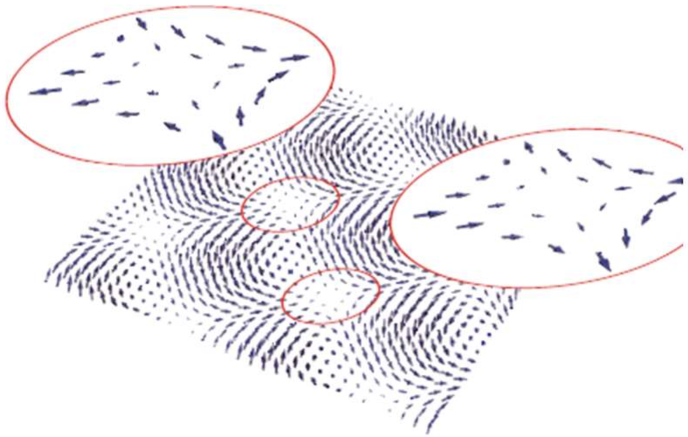

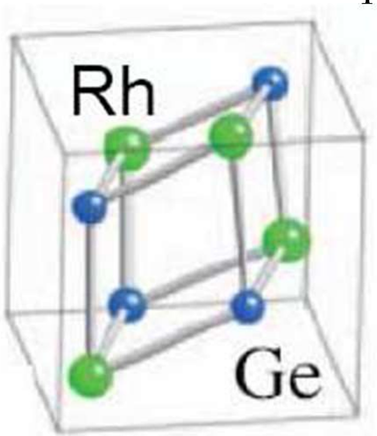


The hedgehogs and anti-hedgehogs lattice

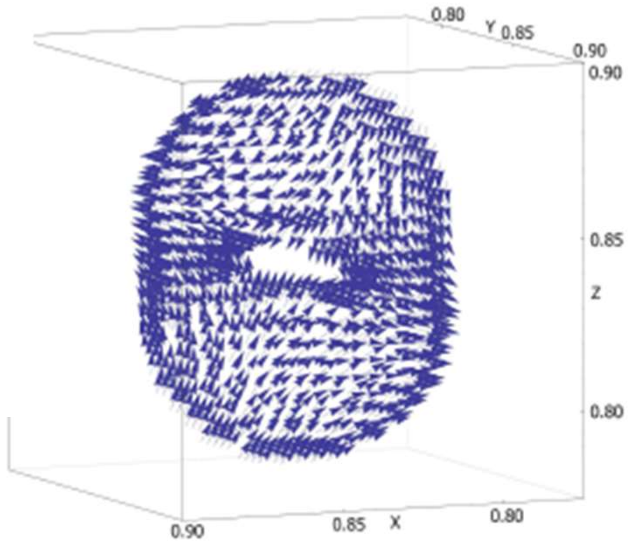


**Zero-energy Bound States in Nodal Topological Lattice**

Soo-Yong Lee and Jung Hoon Han*

PhysRevB.91,245121 (2014)

In two dimensions, superposition of two orthogonally propagating spirals results in the meron-anti-meron (MM) lattice where nodes (points of vanishing magnetization) form a periodic array.

Toroidal distribution of Ge-atom magnetization at one-half of the maximum absolute magnetization . The atom is at u, u, u u(Ge) = 0.83368 position.
In three dimensions, multiple spiral phases are equivalent to a lattice of hedgehogs and anti-hedgehogs (HH) realizing simple cubic, or other crystal symmetries.

# $UGe_2$ – URhGe (UCoGe) - RhGe

forming the spin-triplet state of Cooper pairs

the mixed spin-singlet and spin-triplet states

***$T_C/T_s \approx 30/\,0.8 = 37.5$***

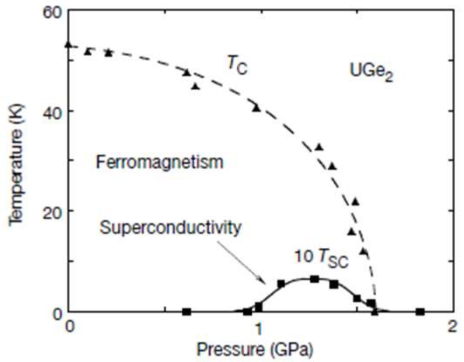


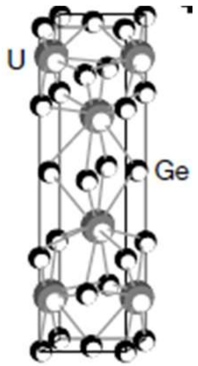


$ZrGa_2$-type structure

*Cmmm*

***$T_C/T_s \approx 9.6/\,0.25 = 38.4$***

$T_{Curie}$ = 9.5 K  ($T_{Curie} \approx$ 3 K)

$M_0$ = 0.4 $\mu_B$  ($M_0$ = 0.05 $\mu_B$)

$T_{SC}$ = 0.25 K  ($T_{SC}$ = 0.7 K)

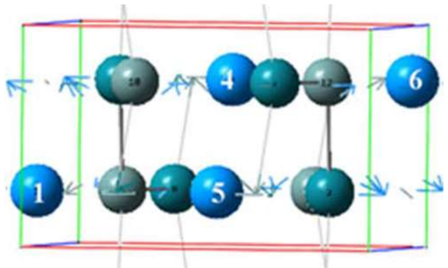

TiNiSi-type structure

the space group *Pnma*

***$T_C/T_s \approx 145/\,4 = 36.3$***

$T_{Curie}$ = 145 K

$M_0 \approx 0.001\ \mu_B$

$T_{SC}$ = 4.0 K

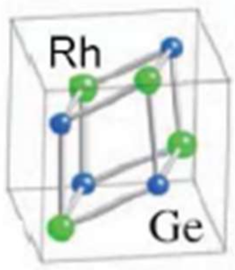


FeSi-type structure

space group $P2_13$

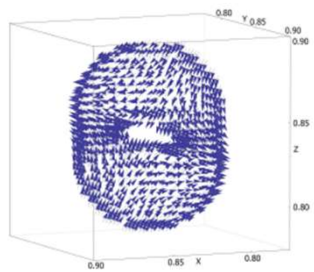

СПАСИБО